

Mechanistic Study on Complexation-Induced *Spring and Hover* Dissolution Behavior of Ibuprofen-Nicotinamide Cocrystal

Yuanfeng Wei ^{#,†}, Li Zhang ^{#,‡}, Ningning Wang [‡], Peiya Shen [†], Haitao Dou [†], Kun Ma [†],
Yuan Gao [†], Jianjun Zhang ^{*‡}, Shuai Qian ^{*†}

[†] School of Traditional Chinese Pharmacy, China Pharmaceutical University, Nanjing,
211198, P.R. China

[‡] School of Pharmacy, China Pharmaceutical University, Nanjing, 211198, P.R. China

1. Solid state characterizations of IBU-NIC cocrystal

Methods

Differential scanning calorimetry (DSC) and thermal gravimetric analysis (TGA)

Thermal analyses of DSC and TGA were carried out using a differential scanning calorimeter (Netzsch DSC 204 F1 Phoenix, Germany) and thermal gravimetric analyzer (Netzsch TG 209C, Germany), respectively. For DSC analysis, the temperature and cell constants were calibrated using indium. Samples of about 3-5 mg crimped in a non-hermetic aluminum DSC pan were heated from 40 to 250 °C at a heating rate of 10 °C/min. Data analysis was performed using Netzsch-Proteus software (version 4.2). For TGA, the system was calibrated using alumel and iron. Samples of about 3-7 mg were loaded into an aluminum pan and heated in a nitrogen purge with a heating rate of 10 °C/min. Scans were carried out within the temperature range of 30 to 250 °C.

Powder X-ray diffraction (PXRD)

PXRD was performed at ambient temperature using a thermo X'TRA X-ray power diffractometer (Thermo Fisher Scientific Inc., USA) with a Cu-K α radiation ($\lambda = 1.5406$ Å) source. The samples were gently placed in an aluminum holder. The tube voltage and amperage were set at 40 kV and 40 mA, respectively. For each sample, PXRD pattern was collected in the 2θ range of 2-40° with a scanning speed of 4°/min and a step size of 0.02°.

Fourier-Transform infrared spectroscopy (FT-IR)

A Nicolet Impact 410 FT-IR spectrophotometer (Thermo Fisher Scientific Inc., Waltham,

MA, USA) was employed in KBr diffuse reflectance mode for recording the IR spectra of samples. About 2 mg of each sample was mixed with 200 mg KBr and compressed into a tablet. A total of 64 scans were collected (with a spectral resolution of 4 cm^{-1}) over the range of $4000\text{--}400\text{ cm}^{-1}$.

Results

DSC and TGA

The DSC thermograms of IBU, NIC, physical mixture and IBU-NIC cocrystal are shown in Figure 1A. IBU (Figure 1Aa) and NIC (Figure 1Ab) showed endothermic melting peaks at $79.7\text{ }^{\circ}\text{C}$ (ΔH_m : 28.5 kJ/mol) and $131.5\text{ }^{\circ}\text{C}$ (ΔH_m : 26.5 kJ/mol), respectively. For physical mixture (Figure 1Ac), an initial endothermic peak at $75.2\text{ }^{\circ}\text{C}$ followed by a broad endotherm at $90.8\text{ }^{\circ}\text{C}$ was observed. However, after cocrystallization, IBU-NIC cocrystal exhibited a single sharp endothermic melting peak at $91.1\text{ }^{\circ}\text{C}$ (ΔH_m : 51.4 kJ/mol).

The TGA thermograms of IBU, NIC, physical mixture and IBU-NIC cocrystal are shown in Figure 1B. No weight loss belonging to residual solvent (i.e., ethanol) was detected prior to the melting point of IBU-NIC cocrystal, indicating that the cocrystal was not a cocrystal solvate.

PXRD

PXRD patterns of IBU, NIC, physical mixture and IBU-NIC cocrystal are depicted in Figure 2. IBU and NIC showed characteristic peaks at 2θ values of (6.1° , 12.1° , 20.1° ,

Figure 2a) and (14.7°, 25.8°, 27.3°, Figure 2b), respectively. Overlapped diffraction peaks of IBU and NIC were observed in their physical mixture (Figure 2c). However, the PXRD pattern of IBU-NIC cocrystal, without indicative peaks of IBU and NIC, had the characteristic peaks at 2θ values of 3.1°, 9.3° and 12.5° (Figure 2d).

FT-IR

The FT-IR spectra for the studied samples (IBU, NIC and IBU-NIC cocrystal) are shown in Figure 3. IBU showed characteristic vibration of C=O in carboxyl group at 1720.7 cm^{-1} . Amino group $-\text{NH}_2$, carbonyl group C=O and C–N bond presenting in primary amide of NIC showed vibration absorptions at (3366.6 and 3158.9) cm^{-1} , 1680.2 cm^{-1} , and 1396.0 cm^{-1} , respectively; C=N ring stretching vibration in pyridine ring of NIC exhibited the absorption peak at 1484.7 cm^{-1} , which were consistent with previous reports.^{1,2} After cocrystallization, typical C=O stretching vibration of IBU in IBU-NIC cocrystal demonstrated a significant bathochromic shift (1720.7 \rightarrow 1706.5 cm^{-1}); in addition, the $-\text{NH}_2$ group and C=O group of NIC in cocrystal exhibited hypsochromic shifts (3366.6 \rightarrow 3401.0 cm^{-1} and 3158.9 \rightarrow 3180.6 cm^{-1}) and slight bathochromic shift (1680.2 \rightarrow 1674.9 cm^{-1}), respectively. Moreover, the C=N double bond on pyridine ring of NIC in cocrystal displayed a significant hypsochromic shift (1484.7 \rightarrow 1514.4 cm^{-1}), while the shift of C–N single bond in amide group was negligible.

Discussion

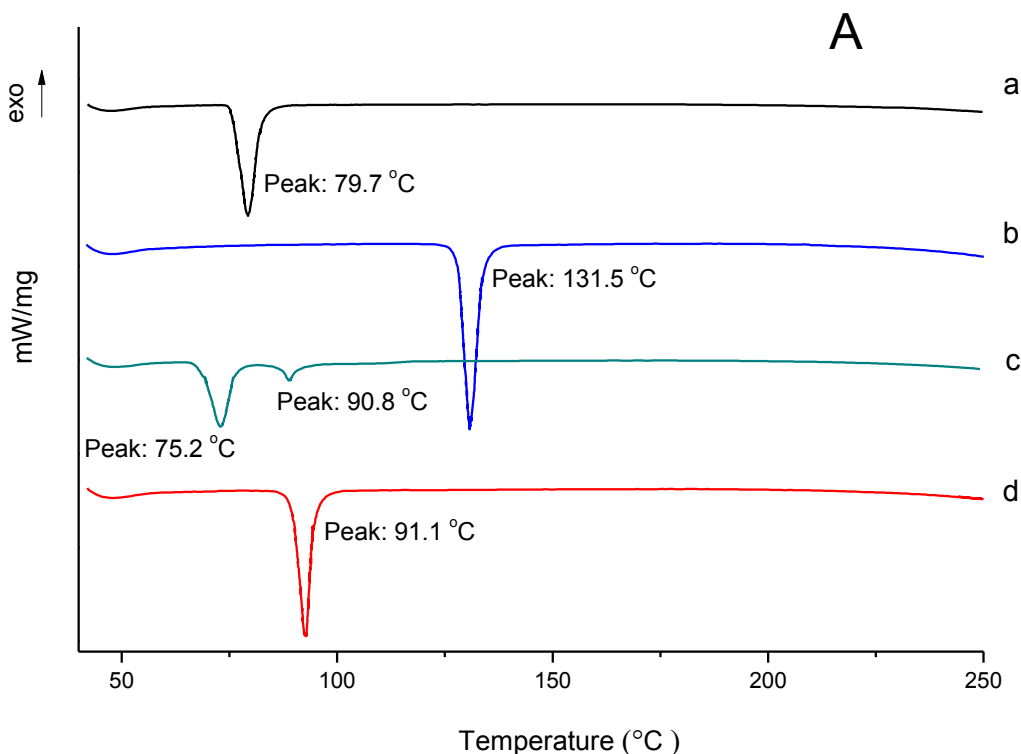
In the present study, slow evaporation method was employed to fabricate the IBU-NIC

cocrystal. The evaporation product of ethanol solution containing equal mole of IBU and NIC show a single melting peak (91.1 °C) between those of individual components, which was distinguishable from the physical mixture with two broad endothermic peaks, suggesting the formation of new cocrystal phase. The melt point of the prepared cocrystal also agreed with the previously reported.^{1,3,4} For physical mixture, an endothermic peak at 75.2 °C lower than both melting points of IBU and NIC was observed, which was ascribed to the probable formation of eutectics;¹ the followed small and broad endotherm at 90.8 °C may be the melting behavior of the *in situ* formed eutectics. On the other hand, compared to single IBU and NIC crystal, the prepared IBU-NIC cocrystal exhibited a unique PXRD pattern with characteristic peaks at 3.1°, 9.3° and 12.5°, which was consistent with reported IBU-NIC cocrystals prepared by fusion method², rotary solvent evaporation¹ and wet milling⁵.

For the original NIC crystal, the neighboring molecules were connected together with chain-structure intermolecular hydrogen bond between -NH₂ and C=O in amino group.¹ After cocrystallization, significant positive shifts (+21.7 and +34.4 cm⁻¹) in -NH₂ and a marginal negative shift (-5.3 cm⁻¹) in C=O of amide group in NIC were observed (Figure S3). In addition, C=N double bond on pyridine ring of NIC also demonstrated a (+29.7 cm⁻¹) shift. Meanwhile, the typical C=O vibration of IBU in cocrystal exhibited a significant negative shift (-14.2 cm⁻¹). The vibration frequency shifts of these polar groups were attributed to the changes of molecular dipole moments, which was probably accounted by the formation of new intermolecular interactions such as hydrogen bonds.⁶

Berry *et al.* reported the single crystal structure of IBU-NIC cocrystal, in which IBU and NIC molecules formed four-membered molecular assemblies. In each assembly, the central part consisted of a NIC dimer to which IBU molecules attached through O–H...N=C bonds (between the carboxylic acid moiety of IBU and the pyridine group of NIC) in the peripheral part.¹ The corresponding groups of IBU and NIC that exhibited vibration changes in FT-IR spectra after cocrystallization (Figure 3) were well agreed with the reported synthon connections in single crystal structure of IBU-NIC cocrystal.

Figure 1. (A) DSC and (B) TGA thermograms of (a) IBU, (b) NIC, (c) physical mixture of IBU and NIC at equal molar ratio, and (d) IBU-NIC cocrystal



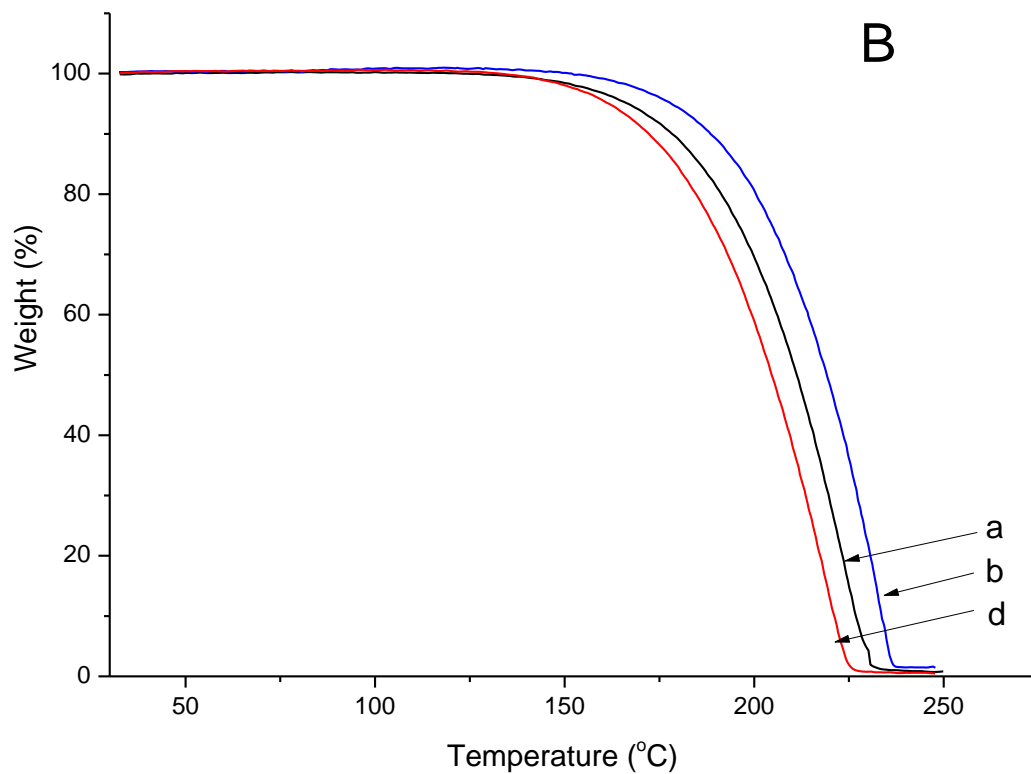


Figure 2. PXRD patterns of (a) IBU, (b) NIC, (c) physical mixture, and (d) IBU-NIC cocrystal

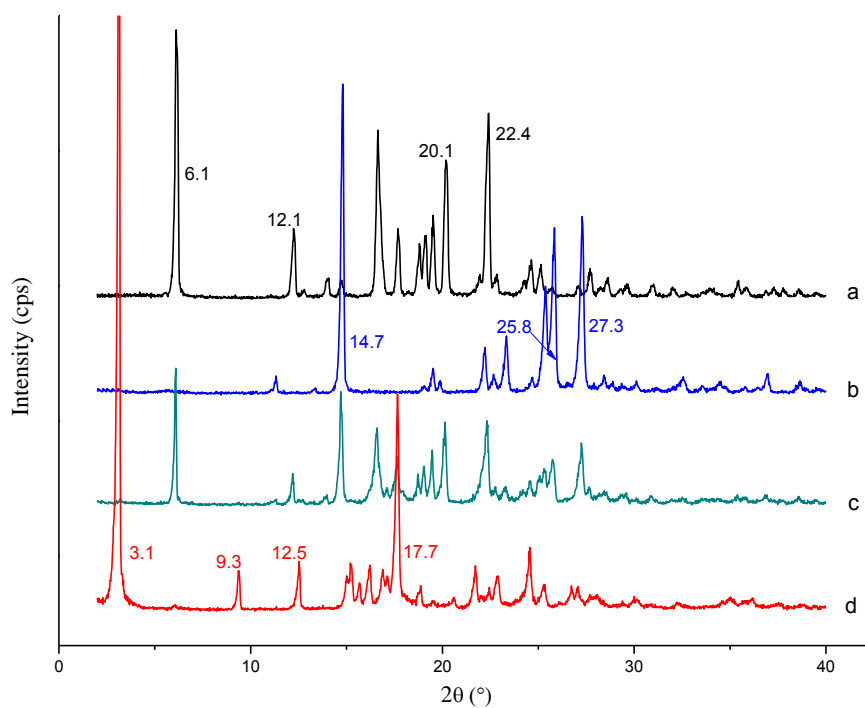
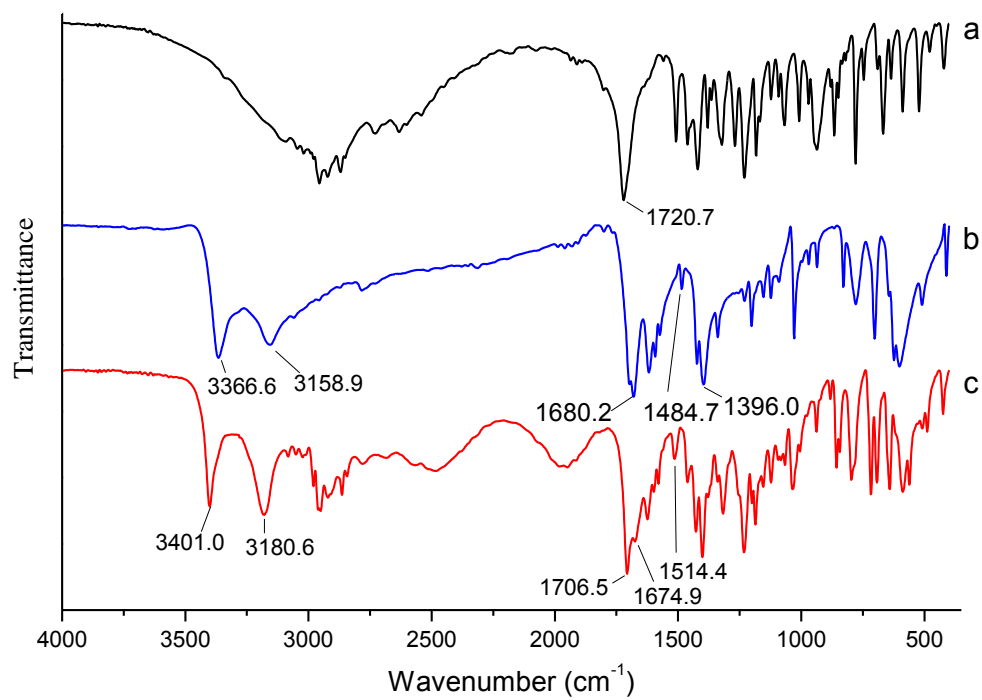
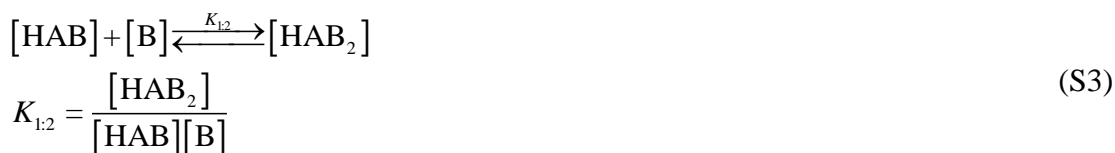


Figure 3. FTIR spectra of (a) IBU, (b) NIC and (c) IBU-NIC cocrystal



2. Equation derivation of cocrystal solubility

IBU-NIC cocrystal-solution equilibria are described by cocrystal dissociation, IBU ionization and solution complexation, the equilibria are expressed as follow:



Where HA represents IBU and B represents NIC. K_{sp} is the solubility product of the cocrystal, $K_{1:1}$ and $K_{1:2}$ are the complexation constants and K_{a} is the acid-ionization constant.

$$[\text{HAB}] = K_{1:1} [\text{HA}][\text{B}] \quad (\text{S5})$$

$$[\text{HAB}_2] = K_{1:2} K_{1:1} [\text{HA}][\text{B}][\text{B}] = K_{1:2} K_{1:1} [\text{HA}][\text{B}]^2 \quad (\text{S6})$$

The total drug analytical concentration is the sum of the ionized and non-ionized species, which is given by:

$$[\text{A}]_{\text{T}} = [\text{HA}] + [\text{A}^-] + [\text{HAB}] + [\text{HAB}_2] \quad (\text{S7})$$

While for unionizable co-former, the total concentration is described as:

$$[\text{B}]_{\text{T}} = [\text{B}] + [\text{HAB}] + 2[\text{HAB}_2] \quad (\text{S8})$$

According to eq (S4 - S6), total drug and co-former concentration could be expressed

as follow:

$$\begin{aligned}
[A]_T &= [HA] + [HA] \frac{K_a}{[H^+]} + K_{1:1} [HA][B] + K_{1:1} K_{1:2} [HA][B]^2 \\
&= [HA] \left(1 + \frac{K_a}{[H^+]} \right) + K_{1:1} [HA] \frac{K_{sp}}{[HA]} + K_{1:1} K_{1:2} [HA] \frac{K_{sp}^2}{[HA]^2} \\
&= [HA] \left(1 + \frac{K_a}{[H^+]} \right) + K_{1:1} K_{sp} + K_{1:1} K_{1:2} \frac{K_{sp}^2}{[HA]}
\end{aligned} \tag{S9}$$

$$\begin{aligned}
[B]_T &= \frac{K_{sp}}{[HA]} + K_{1:1} [HA] \frac{K_{sp}}{[HA]} + 2K_{1:1} K_{1:2} [HA] \frac{K_{sp}^2}{[HA]^2} \\
&= \frac{K_{sp}}{[HA]} + K_{1:1} K_{sp} + 2K_{1:1} K_{1:2} \frac{K_{sp}^2}{[HA]}
\end{aligned} \tag{S10}$$

When cocrystal is in equilibrium with solutions of a stoichiometry equal to that of the cocrystal, then the solubility of cocrystal is equal to the total concentration of its components:⁷

$$S_{\text{cocrystal}} = [A]_T = [B]_T \tag{S11}$$

$$[HA] \left(1 + \frac{K_a}{[H^+]} \right) + K_{1:1} K_{sp} + K_{1:1} K_{1:2} \frac{K_{sp}^2}{[HA]} = \frac{K_{sp}}{[HA]} + K_{1:1} K_{sp} + 2K_{1:1} K_{1:2} \frac{K_{sp}^2}{[HA]} \tag{S12}$$

The expression is rewritten as:

$$[HA] \left(1 + \frac{K_a}{[H^+]} \right) = \frac{K_{sp}}{[HA]} + K_{1:1} K_{1:2} \frac{K_{sp}^2}{[HA]} = \frac{1}{[HA]} (K_{sp} + K_{1:1} K_{1:2} K_{sp}^2) \tag{S13}$$

$$[HA]^2 \left(1 + \frac{K_a}{[H^+]} \right) = K_{sp} + K_{1:1} K_{1:2} K_{sp}^2 \tag{S14}$$

Therefore:

$$[HA] = \sqrt{\frac{K_{sp} + K_{1:1} K_{1:2} K_{sp}^2}{1 + \frac{K_a}{[H^+]}}} \tag{S15}$$

$[B]_T$ can be written as:

$$\begin{aligned}
[B]_T &= \frac{K_{sp}}{\sqrt{\frac{K_{sp} + K_{1:1}K_{1:2}K_{sp}^2}{1 + \frac{K_a}{[H^+]}}} + K_{1:1}K_{sp} + 2K_{1:1}K_{1:2}} \frac{K_{sp}^2}{\sqrt{\frac{K_{sp} + K_{1:1}K_{1:2}K_{sp}^2}{1 + \frac{K_a}{[H^+]}}} \\
&= \frac{K_{sp}^2}{\sqrt{\frac{K_{sp}(1 + K_{1:1}K_{1:2}K_{sp})}{1 + \frac{K_a}{[H^+]}}} + K_{1:1}K_{sp} + 2K_{1:1}K_{1:2}} \sqrt{\frac{K_{sp}^4 \left(1 + \frac{K_a}{[H^+]}\right)}{K_{sp}(1 + K_{1:1}K_{1:2}K_{sp})}} \\
&= \sqrt{\frac{K_{sp} \left(1 + \frac{K_a}{[H^+]}\right)}{1 + K_{1:1}K_{1:2}K_{sp}}} + K_{1:1}K_{sp} + 2K_{1:1}K_{1:2}} \sqrt{\frac{K_{sp} \left(1 + \frac{K_a}{[H^+]}\right)}{1 + K_{1:1}K_{1:2}K_{sp}}} \\
&= (1 + 2K_{1:1}K_{1:2}K_{sp}) \sqrt{\frac{K_{sp} \left(1 + \frac{K_a}{[H^+]}\right)}{1 + K_{1:1}K_{1:2}K_{sp}}} + K_{1:1}K_{sp} \tag{S16}
\end{aligned}$$

(1) If $K_{1:1} = 0$, then

$$S_{\text{cocystal}} = [B]_T = \sqrt{K_{sp} \left(1 + \frac{K_a}{[H^+]}\right)} \tag{S17}$$

Which is agreed with S_{cocystal} reported by Good and Rodriguez-Hornedo¹ that only considered the dissociation and ionization of cocystal in solution;

(2) If $K_{1:1} \neq 0, K_{1:2} = 0$, then

$$S_{\text{cocystal (1:1complex)}} = [B]_T = \sqrt{K_{sp} \left(1 + \frac{K_a}{[H^+]}\right)} + K_{1:1}K_{sp} \tag{S18}$$

$K_{1:1}K_{sp} > 0$, therefore, $S_{\text{cocystal (1:1complex)}} > S_{\text{cocystal}}$;

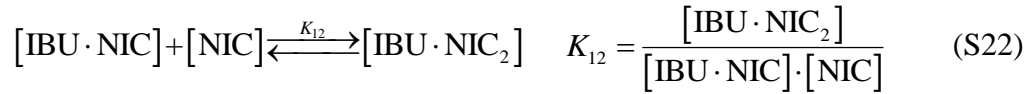
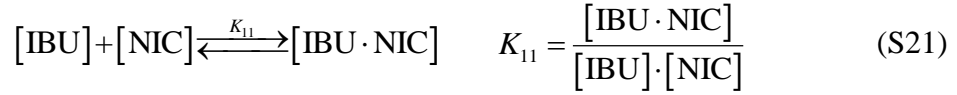
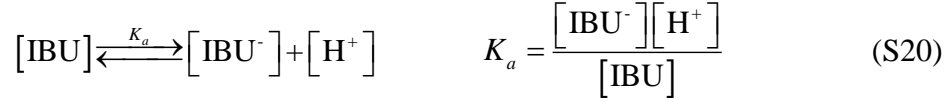
(3) If $K_{1:1} \neq 0, K_{1:2} \neq 0$, then

$$\begin{aligned}
S_{\text{cocrystal (1:1+1:2 complex)}} &= (1 + 2K_{1:1}K_{1:2}K_{\text{sp}}) \sqrt{\frac{K_{\text{sp}} \left(1 + \frac{K_{\text{a}}}{[\text{H}^+]}\right)}{1 + K_{1:1}K_{1:2}K_{\text{sp}}}} + K_{1:1}K_{\text{sp}} \\
&= \sqrt{\left(1 + \frac{K_{\text{a}}}{[\text{H}^+]}\right) \frac{K_{\text{sp}} (1 + 2K_{1:1}K_{1:2}K_{\text{sp}})^2}{1 + K_{1:1}K_{1:2}K_{\text{sp}}}} + K_{1:1}K_{\text{sp}}
\end{aligned} \tag{S19}$$

Because $1 + \frac{K_{\text{a}}}{[\text{H}^+]} \geq 1$ and $\frac{(1 + 2K_{1:1}K_{1:2}K_{\text{sp}})^2}{1 + K_{1:1}K_{1:2}K_{\text{sp}}} \geq 1$, then

$$S_{\text{cocrystal (1:1+1:2 complex)}} > S_{\text{cocrystal (1:1 complex)}} > S_{\text{cocrystal}}$$

3. Equations derivation of calculating complexation constants by considering the influences of pH values in solution



eq. (S20), eq. (S21) and eq. (S22) could be written as

$$[\text{IBU}^-] = \frac{K_a}{[\text{H}^+]} [\text{IBU}] \quad (\text{S23})$$

$$[\text{IBU} \cdot \text{NIC}] = K_{11} [\text{IBU}] \cdot [\text{NIC}] \quad (\text{S24})$$

$$[\text{IBU} \cdot \text{NIC}_2] = K_{12} [\text{IBU} \cdot \text{NIC}] \cdot [\text{NIC}] \quad (\text{S25})$$

The total IBU concentration in solution could be expressed as

$$[\text{IBU}_{\text{total}}] = [\text{IBU}] + [\text{IBU}^-] + [\text{IBU} \cdot \text{NIC}] + [\text{IBU} \cdot \text{NIC}_2] \quad (\text{S26})$$

Substituting eq. (S23), eq. (S24) and eq. (S25) into eq. (S26) gives the following:

$$[\text{IBU}_{\text{total}}] = [\text{IBU}] + \frac{K_a}{[\text{H}^+]} [\text{IBU}] + K_{11} [\text{IBU}] \cdot [\text{NIC}] + K_{12} [\text{IBU} \cdot \text{NIC}] \cdot [\text{NIC}] \quad (\text{S27})$$

The total NIC concentration in solution could be expressed as

$$[\text{NIC}_{\text{total}}] = [\text{NIC}] + [\text{IBU} \cdot \text{NIC}] + 2[\text{IBU} \cdot \text{NIC}_2] \quad (\text{S28})$$

or

$$[\text{NIC}] = [\text{NIC}_{\text{total}}] - [\text{IBU} \cdot \text{NIC}] - 2[\text{IBU} \cdot \text{NIC}_2] \quad (\text{S29})$$

Substituting eq. (S26) into eq. (S29) gives the following:

$$[\text{NIC}] = [\text{NIC}_{\text{total}}] + [\text{IBU} \cdot \text{NIC}] - 2([\text{IBU}_{\text{total}}] - [\text{IBU}] - [\text{IBU}^-]) \quad (\text{S30})$$

Substituting eq. (S23) and eq. (S24) into eq. (S30) gives the following:

$$[\text{NIC}] = \frac{[\text{NIC}_{\text{total}}] - 2 \left\{ [\text{IBU}_{\text{total}}] - [\text{IBU}] \cdot \left(1 + \frac{K_a}{[\text{H}^+]} \right) \right\}}{1 - K_{11} [\text{IBU}]} \quad (\text{S31})$$

$$\text{Let } a = [\text{NIC}_{\text{total}}] - 2 \left\{ [\text{IBU}_{\text{total}}] - [\text{IBU}] \cdot \left(1 + \frac{K_a}{[\text{H}^+]} \right) \right\} \quad (\text{S32})$$

then,

$$[\text{NIC}] = \frac{a}{1 - K_{11} [\text{IBU}]} \quad (\text{S33})$$

Substituting eq. (S31) and eq. (S32) into eq. (S27) gives the following:

$$[\text{IBU}_{\text{total}}] = [\text{IBU}] + \frac{K_a}{[\text{H}^+]} [\text{IBU}] + K_{11} [\text{IBU}] \cdot \frac{a}{1 - K_{11} [\text{IBU}]} + K_{11} K_{12} [\text{IBU}] \frac{a^2}{(1 - K_{11} [\text{IBU}])^2} \quad (\text{S34})$$

or

$$[\text{IBU}_{\text{total}}] - [\text{IBU}] \cdot \left(1 + \frac{K_a}{[\text{H}^+]} \right) = K_{11} [\text{IBU}] \cdot \frac{a}{1 - K_{11} [\text{IBU}]} + K_{11} K_{12} [\text{IBU}] \frac{a^2}{(1 - K_{11} [\text{IBU}])^2} \quad (\text{S35})$$

or

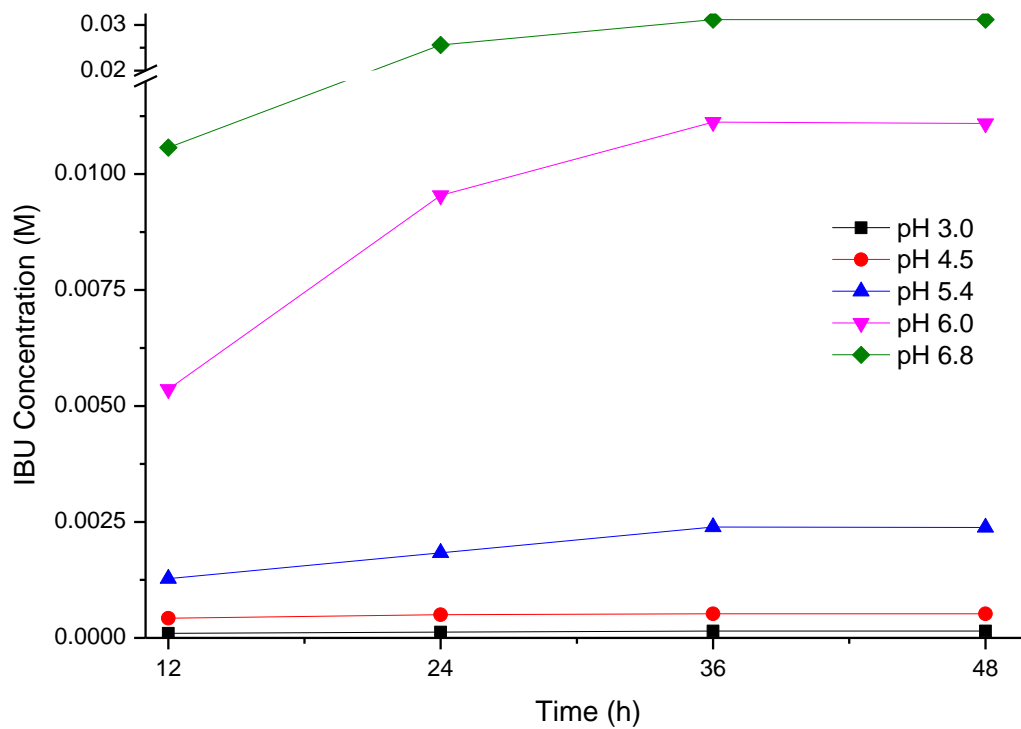
$$\frac{[\text{IBU}_{\text{total}}] - [\text{IBU}] \cdot \left(1 + \frac{K_a}{[\text{H}^+]} \right)}{a} = \frac{K_{11} [\text{IBU}]}{1 - K_{11} [\text{IBU}]} + \frac{K_{11} K_{12} [\text{IBU}] \cdot a}{(1 - K_{11} [\text{IBU}])^2} \quad (\text{S36})$$

Substituting eq. (S32) into eq. (S36) gives the following:

$$\frac{[\text{IBU}_{\text{total}}] - [\text{IBU}] \cdot \left(1 + \frac{K_a}{[\text{H}^+]} \right)}{[\text{NIC}_{\text{total}}] - 2 \left\{ [\text{IBU}_{\text{total}}] - [\text{IBU}] \cdot \left(1 + \frac{K_a}{[\text{H}^+]} \right) \right\}} = \frac{K_{11} [\text{IBU}]}{1 - K_{11} [\text{IBU}]} + \frac{K_{11} K_{12} [\text{IBU}] \cdot \left\{ [\text{NIC}_{\text{total}}] - 2 \left\{ [\text{IBU}_{\text{total}}] - [\text{IBU}] \cdot \left(1 + \frac{K_a}{[\text{H}^+]} \right) \right\} \right\}}{(1 - K_{11} [\text{IBU}])^2}$$

4. Figure S1 showed the concentration-time profiles for equilibrium solubility measurements of crystalline IBU in various aqueous medium.

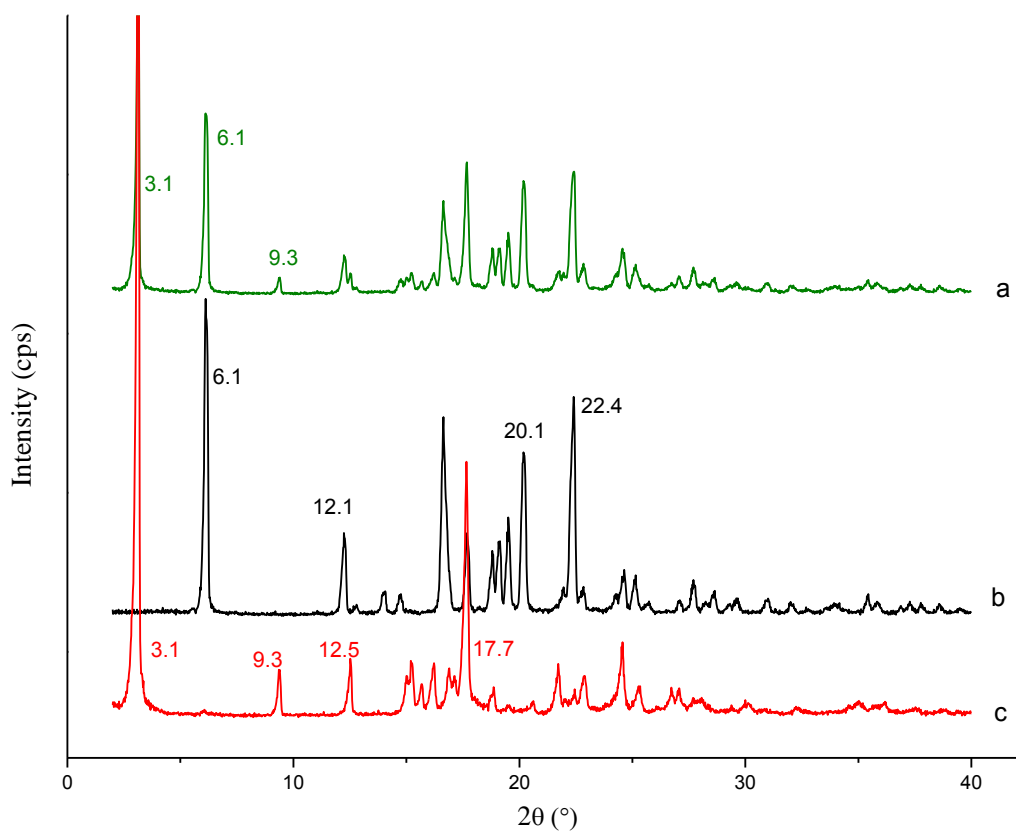
Figure S1



5. Figure S2 represents PXRD pattern of (a) solid residue collected at equilibrium of IBU-NIC cocrystal and IBU during solubility study, (b) IBU crystal and (c) IBU-NIC cocrystal.

The solid phase at equilibrium was examined by PXRD and showed typical PXRD patterns of both IBU and cocrystal, indicating the equilibrium achieved.

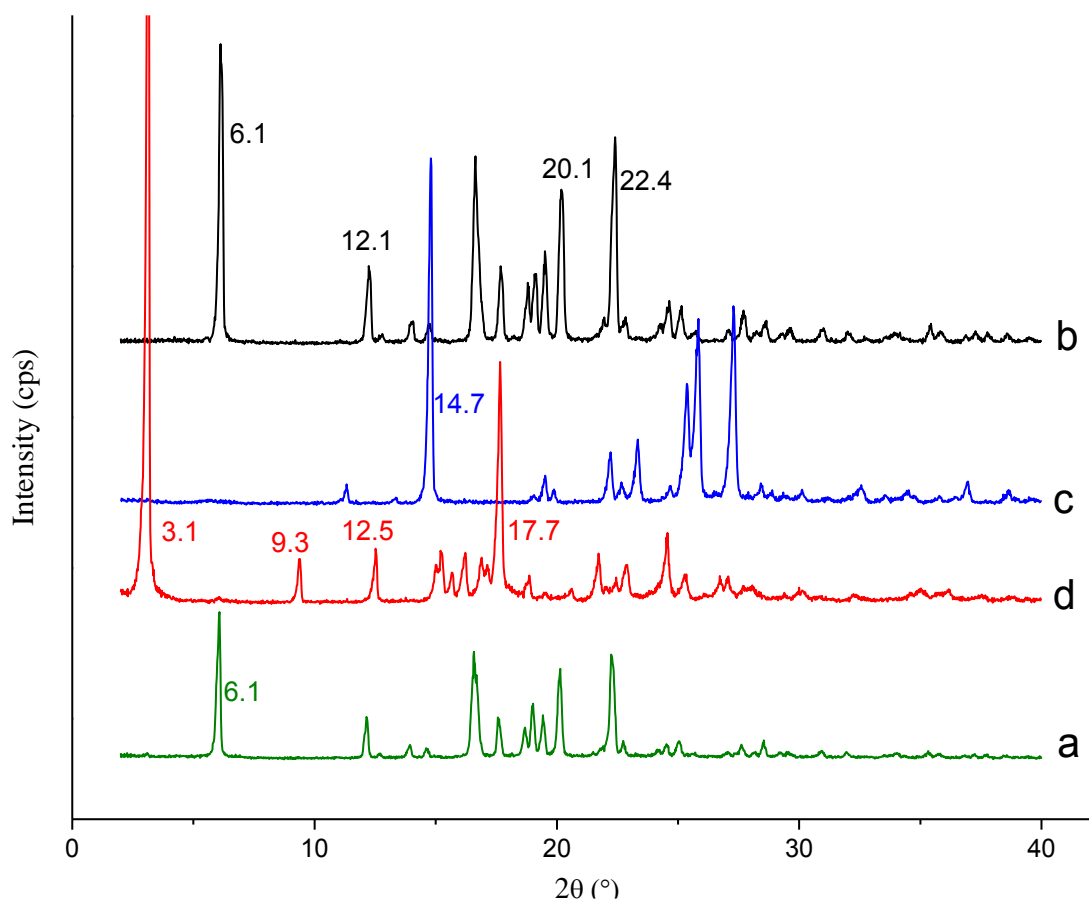
Figure S2



6. Figure S3 represents PXRD pattern of (a) the collected residue solids after phase solubility study in 0.205 M NIC solution, (b) IBU, (c) NIC and (d) IBU-NIC cocrystal

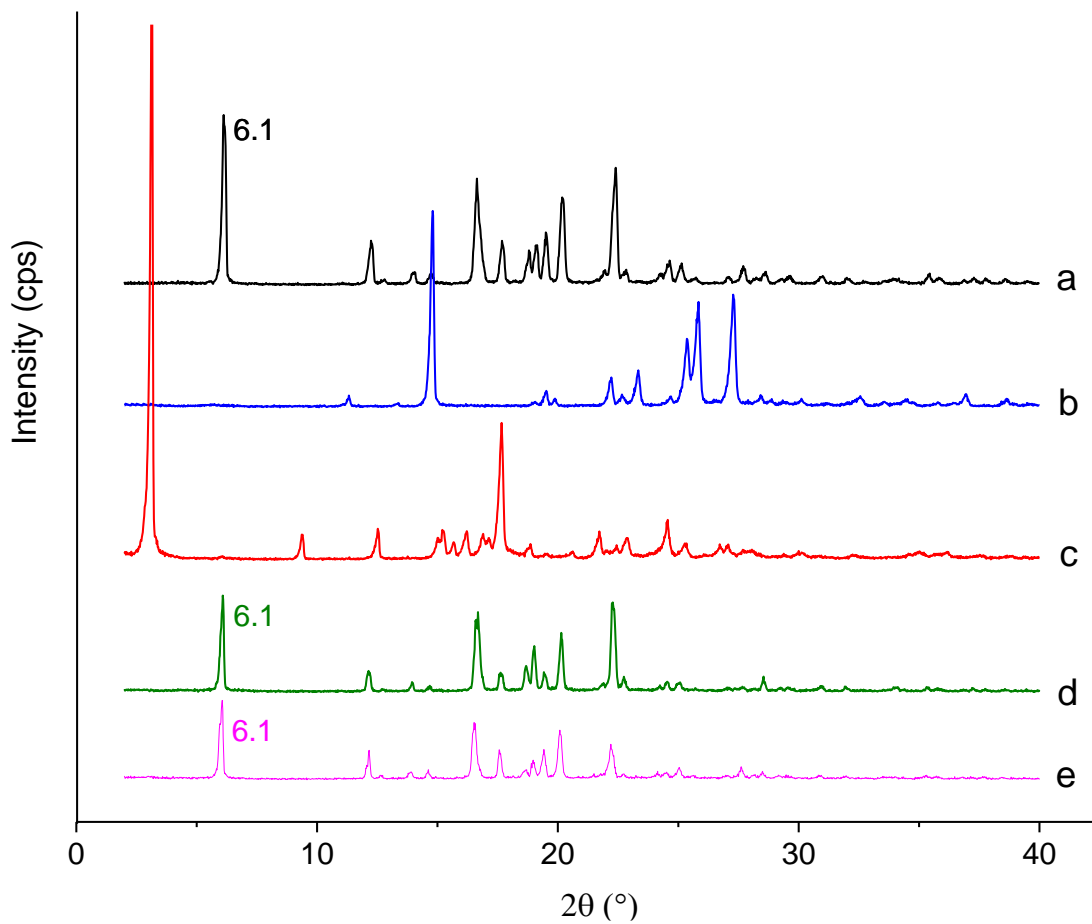
After phase solubility study, the collected residue solids showed typical PXRD pattern of IBU crystal, suggesting the left solid was IBU crystal.

Figure S3



7. Figure S4 represents PXRD patterns of (a) IBU reference, (b) NIC reference, (c) IBU-NIC cocrystal reference, and solid residues after non-sink dissolutions of (d) physical mixture and (e) IBU-NIC cocrystal

Figure S4



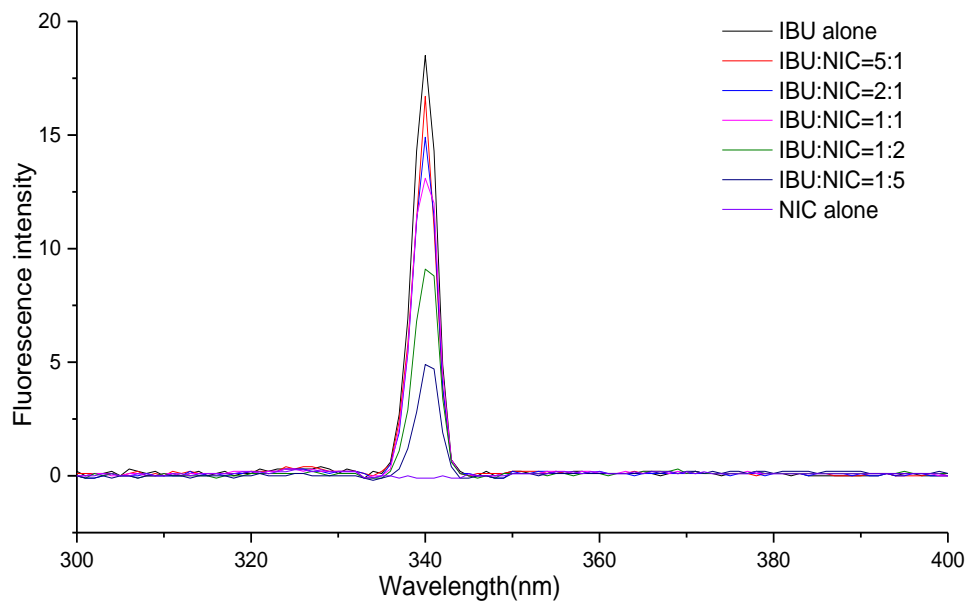
8. Fluorescence quenching of IBU by NIC in solution

All fluorescence spectra were recorded on a RF-6000 fluorescence spectrophotometer (Shimadzu Corporation, Kyoto, Japan) equipped with a xenon flash lamp using 1.0 cm quartz cells. A series of test solutions containing IBU and NIC at the molar ratios of 5:1, 2:1, 1:1, 1:2 and 1:5 were prepared in PBS 6.8 with a fixed IBU concentration at 0.01 M. The fluorescence spectra of the test solutions in the range of 300 to 400 nm were obtained upon an excitation wavelength of 295 nm. Solutions containing 0.01 M of only IBU or NIC were served as controls.

The fluorescence spectra of the studied samples are showed in Figure S4. IBU alone exhibited a strong fluorescence absorption peak at 340 nm, while NIC did not show any fluorescence absorption. After adding NIC in the solution containing 0.01 M IBU, the fluorescence intensity gradually decreased with the increase of NIC dosage (from 5:1 to 1:5 for IBU:NIC), suggesting that NIC could produce a fluorescence quenching effect on IBU.

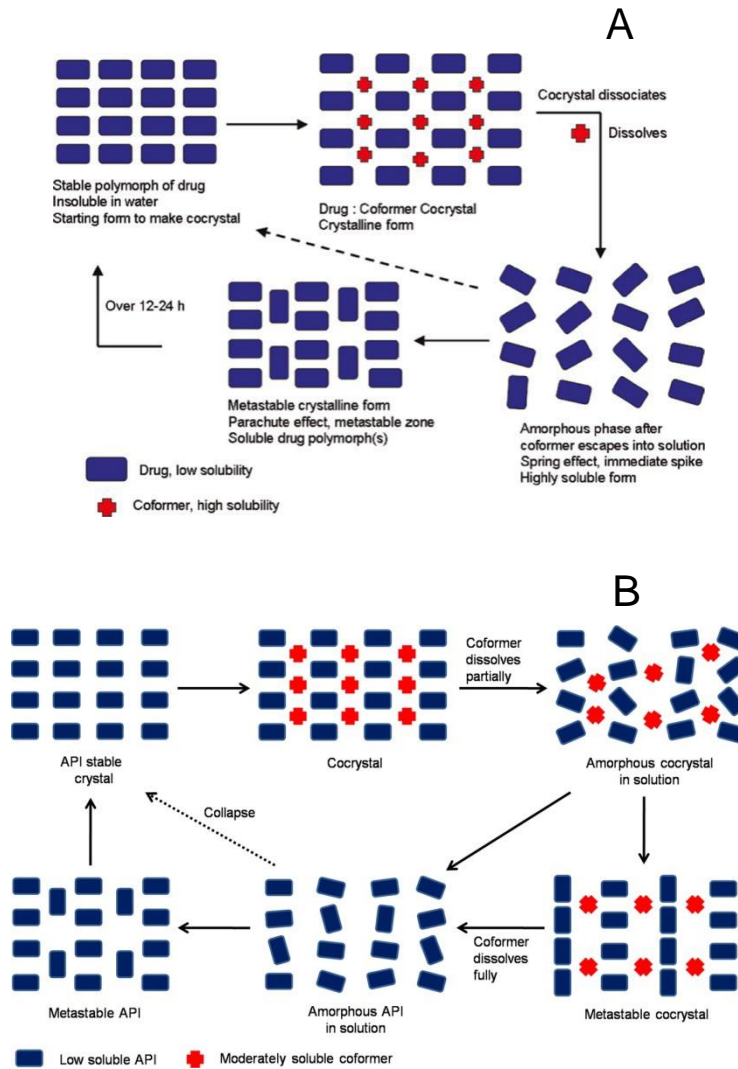
Figure S5 represents Fluorescence spectra of solutions containing 0.01 M IBU, 0.01 M NIC, and 0.01 M IBU with NIC at various molar ratios (5:1, 2:1, 1:1, 1:2 and 1:5)

Figure S5



9. Figure S6 represents schematic diagrams of (A) simple spring and parachute model⁸ and (B) synthon-extended spring and parachute model for cocrystals⁹

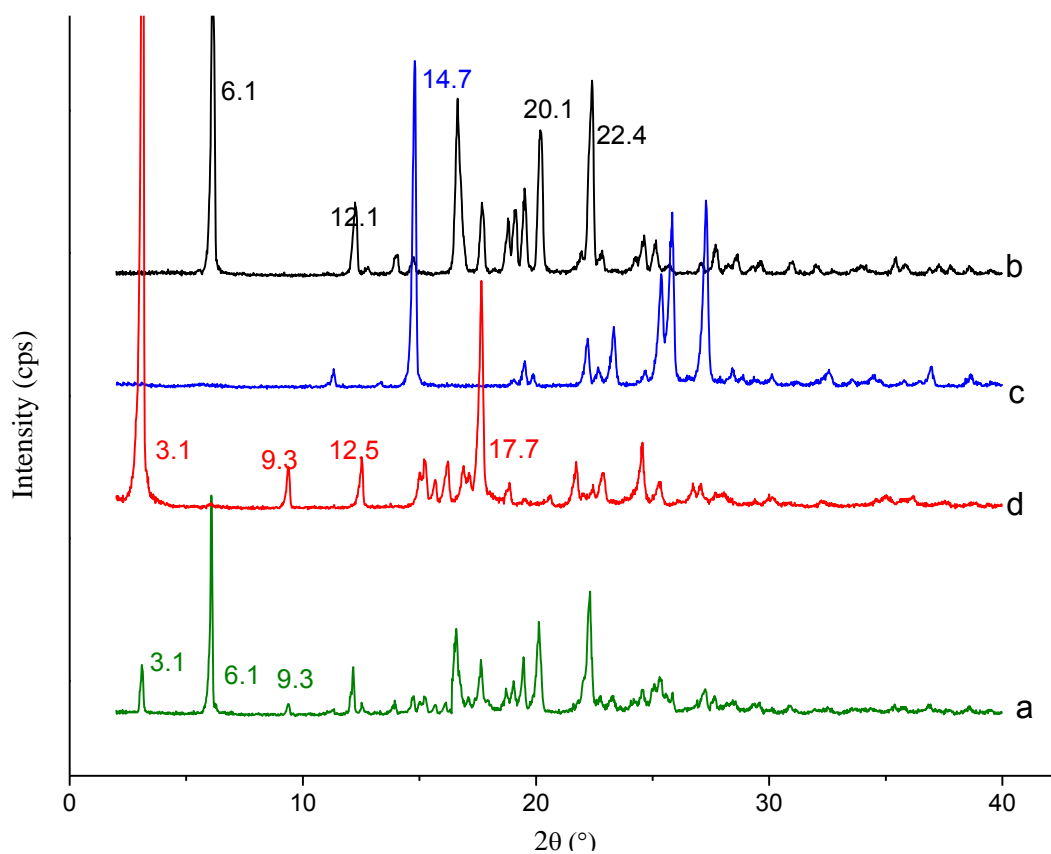
Figure S6



10. Figure S7 represents the PXRD pattern of (a) residue solids after adding excess amount of IBU-NIC cocrystal into water, (b) IBU, (c) NIC and (d) IBU-NIC cocrystal

According to characteristic peaks of IBU (6.1° , 12.1°) and IBU-NIC cocrystal (3.1° , 9.3°), the residue solids (Fig. S7a) contained both IBU and IBU-NIC cocrystal.

Figure S7



11. Figure illustrations for the crystallization process of IBU

Figure S8-S10 were taken under polarized light microscopy (PLM) for the crystallization process of melted IBU, IBU in water and IBU in NIC solution, respectively.

Melted IBU was prepared by placing crystalline IBU in 80 °C oven, followed by transferring it onto glass slide at ambient temperature under PLM. The crystallization process was photographed at various time points (Figure S8).

Crystallization processes of IBU in water (Figure S9) and NIC solution (Figure S10) were conducted by dropping ethanol solution containing high concentration of IBU (10 mg/mL) into ~100 μ L of water or NIC solution (2 mg/mL) via a needle on the glass slide. Photos were taken at various time points under PLM.

Figure S8

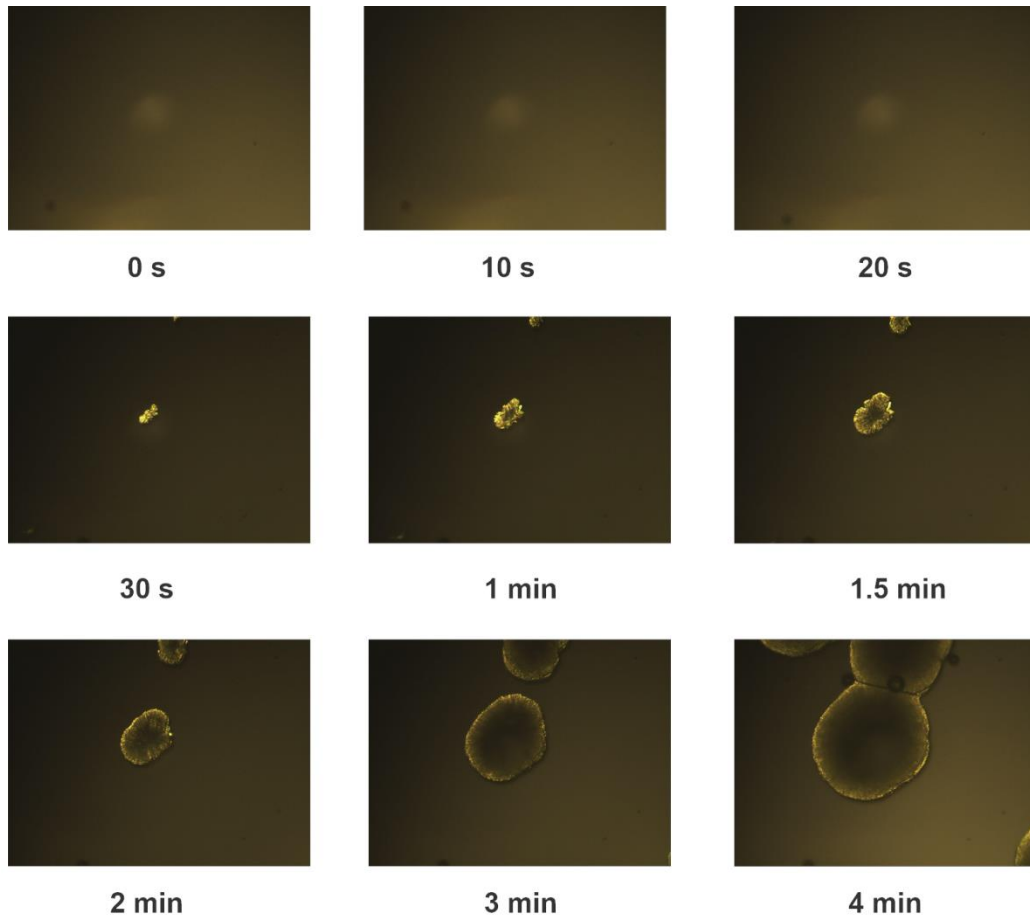


Figure S9

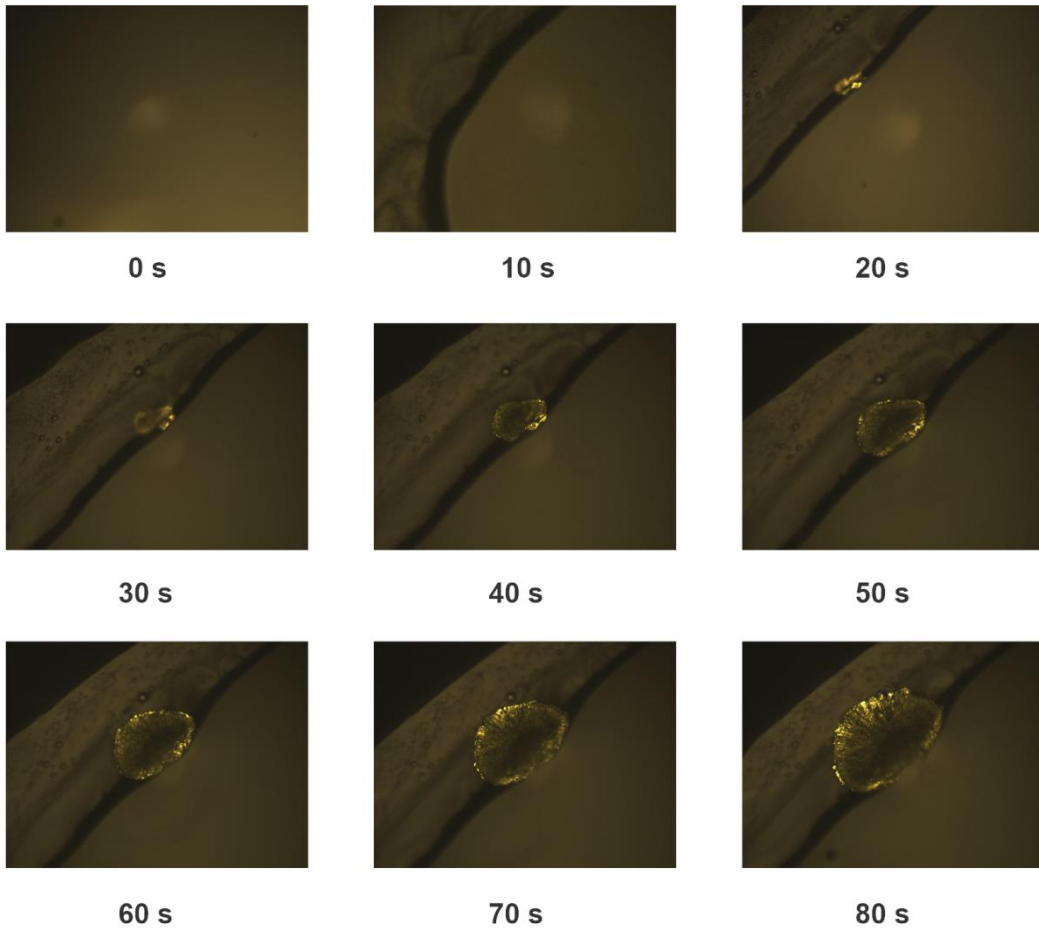
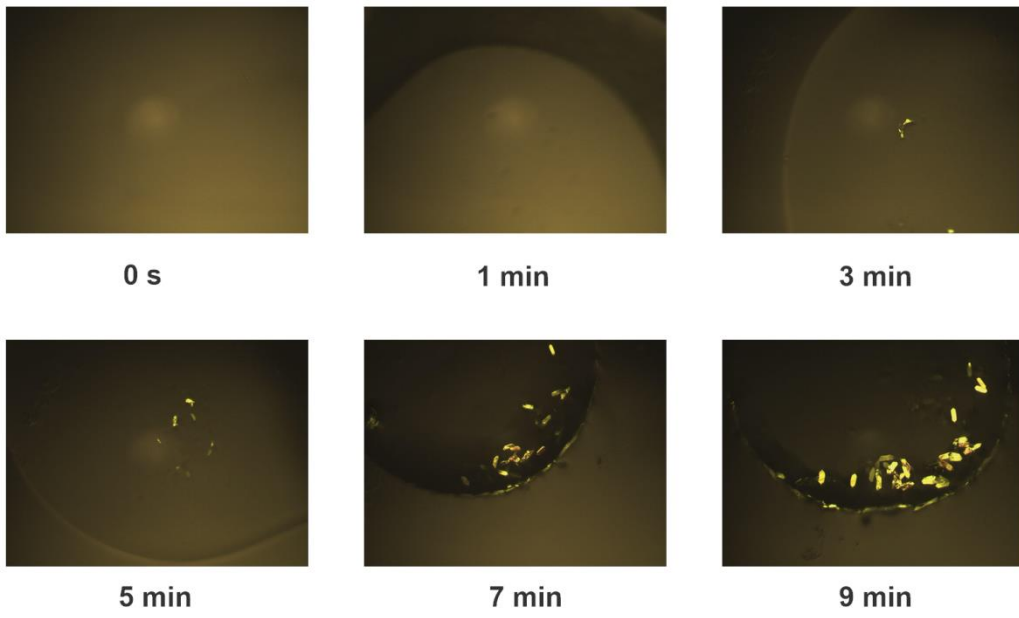


Figure S10



12. The energies of hydrogen bonds in IBU-NIC cocrystal were calculated by Gaussian 09W and Multiwfn software.

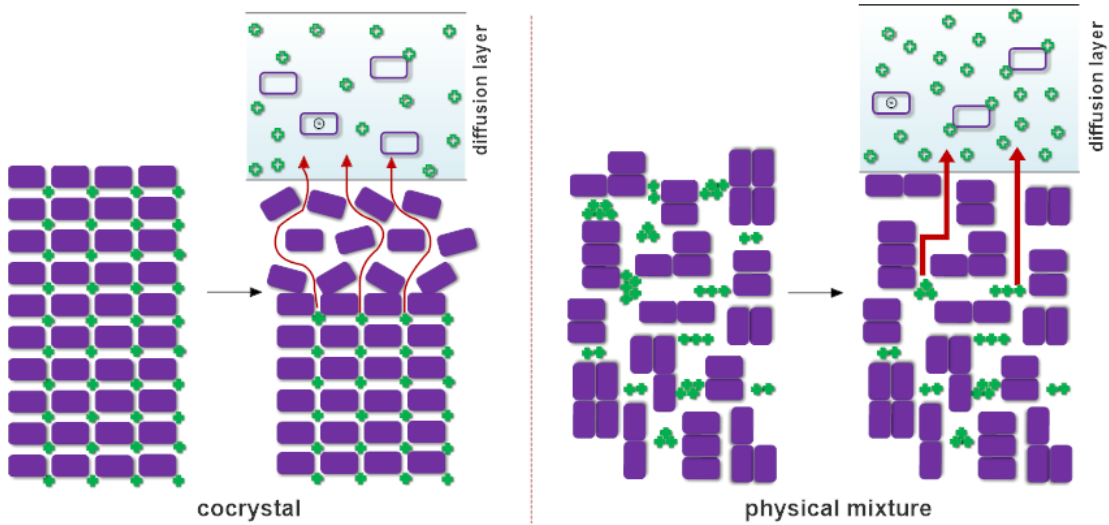
Table S1. Energies of hydrogen bonds in IBU-NIC cocrystal

D-H...A	V_{BCP} (a.u.)	E_{int} (a.u.)	E_{int} (kcal·mol ⁻¹)
O(1)-H(18)...N(2)	-0.03469473083	-0.01734736542	-10.89
N(1)-H(41)...O(6)	-0.01384309840	-0.00692154920	-4.34
N(3)-H(47)...O(5)	-0.01330560085	-0.00665280043	-4.17
O(3)-H(36)...N(4)	-0.03476239132	-0.01738119566	-10.91

Note: V_{BCP} , potential energy density at bond critical point; E_{int} , energy of intermolecular hydrogen bond;
1 a.u.= 627.5095 kcal·mol⁻¹.

13. Figure S11 Proposed pathway of NIC released from cocrystal and physical mixture

Figure S11



References

- (1) Chow, S. F.; Chen, M.; Shi, L.; Chow, A. H.; Sun, C. C. Simultaneously improving the mechanical properties, dissolution performance, and hygroscopicity of ibuprofen and flurbiprofen by cocrystallization with nicotinamide. *Pharm. Res.* **2012**, *29*, 1854-65.
- (2) Ramalingam, S.; Periandy, S.; Govindarajan, M.; Mohan, S. FT-IR and FT-Raman vibrational spectra and molecular structure investigation of nicotinamide: a combined experimental and theoretical study. *Spectrochim. Acta. A. Mol. Biomol. Spectrosc.* **2010**, *75*, 1552-8.
- (3) Berry, D. J.; Seaton, C. C.; Clegg, W.; Harrington, R. W.; Coles, S. J.; Horton, P. N.; Hursthouse, M. B.; Storey, R.; Jones, W.; Friscic, T.; Blagden, N. Applying hot-stage microscopy to co-crystal screening: a study of nicotinamide with seven active pharmaceutical ingredients. *Cryst. Growth Des.* **2008**, *8*, 1697-1712.
- (4) Friscic, T.; Jones, W. Cocrystal architecture and properties: design and building of chiral and racemic structures by solid-solid reactions. *Faraday Discuss.* **2007**, *136*, 167-178.
- (5) Sun, X. W.; Yin, Q. X.; Ding, S. P.; Shen, Z. M.; Bao, Y.; Gong, J. B.; Hou, B. H.; Hao, H. X.; Wang, Y. L.; Wang, J. K.; Xie, C. Solid-liquid phase equilibrium and ternary phase diagrams of ibuprofen-nicotinamide cocrystals in ethanol and ethanol/water mixtures at (298.15 and 313.15) K. *J. Chem. Eng. Data* **2015**, *60*, 1166-1172.
- (6) Larkin, P. J., Chapter 2. Basic principles. In *Infrared and Raman Spectroscopy: Principles and Spectral Interpretation*, Larkin, P. J., Ed. Elsevier: MA, USA, **2011**; pp 7-26.
- (7) Good, D. J.; Rodriguez-Hornedo, N. Solubility advantage of pharmaceutical cocrystals. *Cryst. Growth Des.* **2009**, *9*, 2252-2264.
- (8) Babu, N. J.; Nangia, A. Solubility advantage of amorphous drugs and pharmaceutical cocrystals. *Cryst. Growth Des.* **2011**, *11*, 2662-2679.
- (9) Banik, M.; Gopi, S. P.; Ganguly, S.; Desiraju, G. R. Cocrystal and salt forms of furosemide: solubility and diffusion variations. *Cryst. Growth Des.* **2016**, *16*, 5418-5428.